

Attractive Fermi polarons at nonzero temperature with finite impurity concentration

Hui Hu,¹ Brendan C. Mulkerin,¹ Jia Wang,¹ and Xia-Ji Liu¹

¹Centre for Quantum and Optical Science, Swinburne University of Technology, Melbourne, Victoria 3122, Australia

(Dated: August 14, 2017)

We theoretically investigate how quasi-particle properties of an attractive Fermi polaron are affected by nonzero temperature and finite impurity concentration. By applying both non-self-consistent and self-consistent many-body T -matrix theories, we calculate the polaron energy (including decay rate), effective mass, and residue, as functions of temperature and impurity concentration. The temperature and concentration dependences are weak on the BCS side with a negative impurity-medium scattering length. Toward the strong attraction regime across the unitary limit, we find sizable dependences. In particular, with increasing temperature the effective mass quickly approaches the bare mass and the residue is significantly enhanced. At the temperature $T \sim 0.1T_F$, where T_F is the Fermi temperature of the background Fermi sea, the residual polaron-polaron interaction seems to become attractive. This leads to a notable down-shift in the polaron energy. We show that, by taking into account the temperature and impurity concentration effects, the measured polaron energy in the first Fermi polaron experiment [A. Schirotzek *et al.*, Phys. Rev. Lett. **102**, 230402 (2009)] can be better theoretically explained.

PACS numbers: 67.85.d, 03.75.Kk, 03.75.Mn, 05.30.Rt, 71.70.Ej

I. INTRODUCTION

Over the past two decades ultracold atomic gases have provided an ideal platform to understand the intriguing behavior of quantum many-body systems [1]. The simplest example of an interacting many-body system is a moving impurity immersed in a background medium [2]. In this so-called polaron problem, the interaction between impurity and medium in an ultracold Fermi gas can be tuned arbitrarily by using Feshbach resonances [3]. The motion of the impurity is then addressed by low-energy excitations of the background medium and its fundamental properties are profoundly affected [2]. In the case of fermionic impurity with finite density/concentration, the emergence of Fermi liquid behavior is anticipated [4, 5].

Theoretically, it turns out that the polaron problem can be well approximated by a variational ansatz that includes only one-particle-hole excitations, as proposed by Chevy in 2006 in his seminal work [6]. For a non-interacting single-component Fermi sea as the background medium, and when the impurity-medium scattering length a is tuned to the unitary limit ($a \rightarrow \infty$), Chevy's ansatz predicts a polaron energy of $E_P \simeq -0.607\varepsilon_F$ [6, 7], where ε_F is the Fermi energy of the Fermi sea, which is comparable to the numerically exact diagrammatic Monte Carlo (Diag-MC) result of $E_P = -0.615(1)\varepsilon_F$ [8–10]. This excellent agreement shows the physically important contributions to the polaron energy and may result from a cancellation of the higher-order contributions, as was investigated by the next order calculation with the inclusion of two-particle-hole excitations [11]. The simple variational ansatz was later used to discover repulsive Fermi polarons in a meta-stable upper branch [12] and to describe Bose polarons [13]. At the level of including two-particle-hole excitations, Chevy's ansatz has also been applied to systems with bosonic degrees of freedom, such as a Bose-Einstein condensate

(BEC) [14] or a Bardeen–Cooper–Schrieffer (BCS) superfluid [15, 16]. In those cases, the interplay between polarons and the resulting Efimov trimer was explored [14–17].

Experimentally, the first realization of attractive Fermi polarons was carried out by the group at Massachusetts Institute of Technology (MIT) in 2009 using ${}^6\text{Li}$ atoms [18]. The polaron energy and residue were determined by using radio-frequency (rf) spectroscopy in the vicinity of the unitary limit and the strong attractive BEC regime. The attractive polaron picture was used later to understand the radio-frequency spectrum of a quasi-two-dimensional Fermi gas [19]. The existence of metastable repulsive Fermi polarons was experimentally confirmed in 2012 by immersing ${}^{40}\text{K}$ impurity in a Fermi sea of ${}^6\text{Li}$ atoms near a narrow Feshbach resonance [20], and in two dimensions by using ${}^{40}\text{K}$ atoms [21]. Most recently, a careful analysis of the quasi-particle properties of repulsive Fermi polarons in ${}^6\text{Li}$ systems was performed at the European Laboratory for Non-linear Spectroscopy (LENS), Florence [22]. The experimental observation of attractive and repulsive Bose polarons has also been reported [23, 24].

In these experiments the data was compared with the theoretical predictions of a single impurity at zero temperature [2]. The unavoidable nonzero temperature and finite impurity concentration in real experiments are anticipated to give negligible corrections. However, those corrections have never been carefully examined, except the idealized case of 1D Fermi polarons [25], where the exact solution is available. A possible reason is that the current polaron theory relies heavily on Chevy's variational approach [6], which unfortunately is difficult to extend to nonzero temperature and finite impurity concentration [26].

The purpose of the present work is to address the effects of nonzero temperature and finite impurity concen-

tration for attractive Fermi polarons, by using both non-self-consistent [7, 27–31] and self-consistent T -matrix theories [32–35]. In the limit of zero temperature and a single impurity, the non-self-consistent T -matrix theory is equivalent to Chevy’s variational approach [7, 30]. At weak attractions on the BCS side of the impurity and medium scattering resonance, we find that the effects of nonzero temperature and finite impurity concentration are indeed negligible, confirming the previous anticipation. However, across the resonance and toward the strong attraction regime, a nonzero temperature may significantly reduce the effective mass and enhance the residue of attractive Fermi polarons. The polaron energy also shows a considerable temperature dependence. In particular, at the typical experimental temperatures $T \sim 0.1T_F$, where T_F is the Fermi temperature of the Fermi sea, the polaron-polaron interaction may become attractive, leading to a sizable downshift in the polaron energy, which may be experimentally resolved. Indeed, by taking into account the temperature and impurity concentration effects in our non-self consistent T -matrix theory we find that the measured polaron energy in the first Fermi polaron experiment at MIT [18] could be better theoretically understood.

The paper is set out as follows. In Sect. II we outline the T -matrix theories and methodology, defining the quasi-particle properties of Fermi polarons. In Sect. III we give a brief review of the zero temperature behavior of the Fermi polaron. In Sect. IV we describe the quasi-particle properties of the Fermi polaron at finite temperature. In Sect. V we consider finite impurity density and the Fermi liquid behavior, comparing to experimental results at finite temperature and impurity. Finally, in Sect. VI we summarize our results.

II. MANY-BODY T -MATRIX THEORIES OF ATTRACTIVE FERMI POLARONS

We consider a two-component Fermi gas of mass m with a large spin polarization (i.e., $n_\uparrow = n \gg n_\downarrow$), which is described by the model single channel Hamiltonian [6, 7],

$$H = \sum_{\mathbf{k}} \left[(\epsilon_{\mathbf{k}} - \mu) c_{\mathbf{k}\uparrow}^\dagger c_{\mathbf{k}\uparrow} + (\epsilon_{\mathbf{k}} - \mu_\downarrow) c_{\mathbf{k}\downarrow}^\dagger c_{\mathbf{k}\downarrow} \right] + \frac{U}{V} \sum_{\mathbf{q}, \mathbf{k}, \mathbf{k}'} c_{\mathbf{k}\uparrow}^\dagger c_{\mathbf{q}-\mathbf{k}\downarrow}^\dagger c_{\mathbf{q}-\mathbf{k}'\downarrow} c_{\mathbf{k}'\uparrow}, \quad (1)$$

where $\epsilon_{\mathbf{k}} \equiv \hbar^2 \mathbf{k}^2 / (2m)$, μ and μ_\downarrow are the chemical potentials of spin-up and spin-down atoms, respectively, and $U < 0$ is the bare attractive interatomic interaction strength, to be renormalized in terms of the s -wave scattering length a , according to

$$\frac{1}{U} = \frac{m}{4\pi\hbar^2 a} - \sum_{\mathbf{k}} \frac{m}{\hbar^2 \mathbf{k}^2}. \quad (2)$$

In the large spin polarization limit, we treat the spin-down atoms as impurities and assume that, at the first order of the impurity concentration $x = n_\downarrow/n$, the background medium of spin-up atoms is not affected by interactions. As a result, μ can be taken as the chemical potential of an ideal Fermi gas at low temperatures, $\mu^{(0)}(T) \simeq \varepsilon_F = \hbar^2(6\pi^2 n)^{2/3}/(2m)$, and the thermal Green’s function of spin-up atoms is

$$G_\uparrow^{(0)}(\mathbf{k}, i\omega_m) = \frac{1}{i\omega_m - (\epsilon_{\mathbf{k}} - \mu)}, \quad (3)$$

with fermionic Matsubara frequencies $\omega_m \equiv (2m + 1)\pi k_B T$ for integer m . The impurity chemical potential, $\mu_\downarrow < 0$, and the impurity thermal Green’s function, $G_\downarrow(\mathbf{k}, i\omega_m)$, strongly depend on the interatomic interaction and these effects must be taken into account. For a *single* impurity at *zero* temperature, μ_\downarrow gives the polaron energy E_P [7].

A. Many-body T -matrix theories

We solve the impurity thermal Green’s function

$$G_\downarrow(\mathbf{k}, i\omega_m) = \frac{1}{i\omega_m - (\epsilon_{\mathbf{k}} - \mu_\downarrow) - \Sigma(\mathbf{k}, i\omega_m)} \quad (4)$$

by using the well-established many-body T -matrix theories [36–38], which amount to summing up all the ladder-type diagrams. In this approximation, the self-energy Σ of the impurity atom is given by [7],

$$\Sigma = k_B T \sum_{\mathbf{q}, i\nu_n} G_\uparrow^{(0)}(\mathbf{q} - \mathbf{k}, i\nu_n - i\omega_m) \Gamma(\mathbf{q}, i\nu_n), \quad (5)$$

where the vertex function Γ can be written through the Bethe-Salpeter equation as,

$$\Gamma(\mathbf{q}, i\nu_n) = \frac{1}{U^{-1} + \chi(\mathbf{q}, i\nu_n)}, \quad (6)$$

and the pair propagator $\chi(\mathbf{q}, i\nu_n)$ is

$$\chi = k_B T \sum_{\mathbf{k}, i\omega_m} G_\uparrow^{(0)}(\mathbf{q} - \mathbf{k}, i\nu_n - i\omega_m) G_\downarrow(\mathbf{k}, i\omega_m). \quad (7)$$

Here, $\nu_n \equiv 2n\pi k_B T$ with integer n are the bosonic Matsubara frequencies. Equations (4) to (7) form a closed set of equations, which have to be solved self-consistently. We refer to this set of equations as the self-consistent T -matrix theory, or the “ $G_{0\uparrow}G_{0\downarrow}$ ” theory, according to the structure in the pair propagator. We note that in a strong-coupling theory, the self-consistency does not necessarily guarantee a better or more accurate theory [37, 38]. For the calculation of the energy of attractive Fermi polarons at zero temperature, it is actually more useful to take a non-self-consistent treatment of the many-body T -matrix theory, as suggested by the comparison with numerically exact Diag-MC simulations in three

dimensions [8–11] or exact Bethe ansatz solutions in one dimension [25]. That is, we simply use a non-interacting impurity Green’s function

$$G_{\downarrow}^{(0)}(\mathbf{k}, i\omega_m) = \frac{1}{i\omega_m - (\epsilon_{\mathbf{k}} - \mu_{\downarrow})} \quad (8)$$

in the pair propagator Eq. (7). At zero temperature and in the single-impurity limit, this non-self-consistent T -matrix theory, or “ $G_{0\uparrow}G_{0\downarrow}$ ” theory, exactly recovers Chevy’s variational approach [7].

In this work, we explore both non-self-consistent and self-consistent T -matrix theories, as both of them are not justified in the strong-coupling limit [37, 38] and they may give complementary information on some specific observables of interest. Of course, the self-consistent calculations are much more numerically involved, since the integration over $(\mathbf{q}, i\nu_n)$ in Eq. (5) or $(\mathbf{k}, i\omega_m)$ in Eq. (7) is three-dimensional. To overcome this numerical integration difficulty, we rewrite the self-energy and the pair propagator in real space and in imaginary-time space [32–34]:

$$\Sigma(\mathbf{x}, \tau) = G_{\uparrow}^{(0)}(-\mathbf{x}, -\tau)\Gamma(\mathbf{x}, \tau), \quad (9)$$

and

$$\chi(\mathbf{x}, \tau) = G_{\uparrow}^{(0)}(\mathbf{x}, \tau)G_{\downarrow}(\mathbf{x}, \tau), \quad (10)$$

where in the last equation $G_{\downarrow}(\mathbf{x}, \tau)$ should be replaced with $G_{\downarrow}^{(0)}(\mathbf{x}, \tau)$, if we consider the non-self-consistent T -matrix theory. Thus, it is straightforward to calculate self-energy or pair propagator once we know the Green’s functions and vertex function in real space. The trade-off is that we now need to perform two Fourier transforms, $\mathbf{x} \longleftrightarrow \mathbf{k}$ (or \mathbf{q}) and $\tau \longleftrightarrow i\omega_m$ (or $i\nu_n$) [32–34]. Due to the spatial homogeneity and rotational invariance, all the functions in real space (or momentum space) depend on $x = |\mathbf{x}|$ (or $k = |\mathbf{k}|$) only. Hence, the two Fourier transforms are essentially a two-dimensional integration and can be performed very efficiently. It turns out that the only difficulty in our numerical calculations is the singularities of Green functions and vertex function near $\mathbf{x} = 0$ and $\tau = 0^-$. Fortunately, the same singularities appear in the free Green’s function $G^{(0)}$ or in the first-order iterated vertex function $\Gamma^{(n=1)}$ and thus can be easily taken into account in an analytic way [32, 33].

We note that, at zero temperature in the single impurity limit, both non-self-consistent and self-consistent T -matrix theories have been implemented, as a by-product of the Diag-MC simulations of Fermi polarons [9]. Here we extend these theories to the case of nonzero temperature and finite impurity concentration.

B. Quasi-particle properties of Fermi polarons

Once the impurity thermal Green’s function is known, we may directly extract the quasi-particle properties

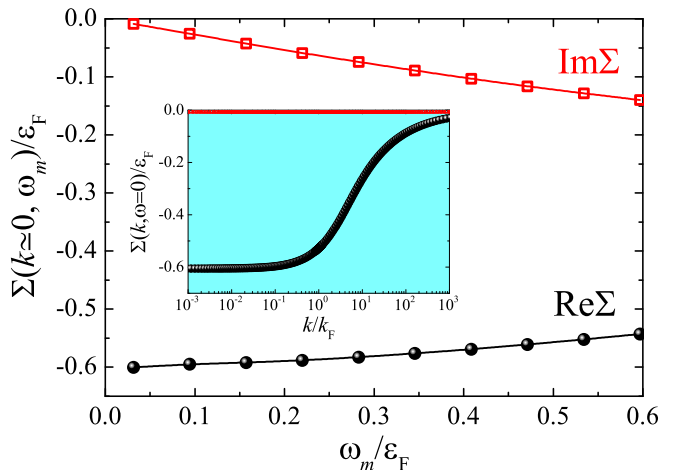


FIG. 1. (color online). The Matsubara frequency dependence of the self-energy of the impurity temperature Green function at very small momentum $k \simeq 0$, calculated by using the non-self-consistent T -matrix theory. Here, we take $1/(k_F a) = 0$ (i.e., the unitary limit), $T = 0.01T_F$ and the impurity chemical potential $\mu_{\downarrow} = -0.607\varepsilon_F$. We extrapolate the data to zero frequency to obtain the retarded self-energy $\Sigma^R(k, i\omega_m \rightarrow \omega = 0)$, which is shown in the inset. The imaginary part of the retarded self-energy $\text{Im}\Sigma^R(\mathbf{k}, 0)$ (red symbols in the inset) is essentially zero due to low temperature.

of Fermi polarons, such as the polaron energy E_P , residue Z , and the effective mass m^* , by approximating the retarded impurity Green’s function $G_{\downarrow}^R(\mathbf{k}, \omega) \equiv G_{\downarrow}(\mathbf{k}, i\omega_m \rightarrow \omega + i0^+)$ in the low-energy and long-wavelength limit as [8, 9],

$$G_{\downarrow}^R = \frac{Z}{\omega - \hbar^2 \mathbf{k}^2 / (2m^*) + \mu_{\downarrow} - E_P + i\gamma/2} + \dots, \quad (11)$$

where γ is the decay rate of the polaron. In the case of a well-defined quasi-particle (i.e., $\gamma \ll |E_P|$), this gives rise to a polaron spectral function $A_{\downarrow}(\mathbf{k}, \omega) = -(1/\pi)\text{Im}G_{\downarrow}(\mathbf{k}, \omega)$ [27, 31],

$$A_{\downarrow}(\mathbf{k}, \omega) = Z\delta\left(\omega + \mu_{\downarrow} - \frac{\hbar^2 \mathbf{k}^2}{2m^*} - E_P\right) + \dots, \quad (12)$$

which can be experimentally measured by using *direct* rf spectroscopy that transfers impurity atoms to a third, non-interacting hyperfine state [18] or by using *inverse* rf spectroscopy that flips initially non-interacting impurity atoms (in the third state) into the strongly interacting polaron state [22]. The explicit expressions for the polaron energy, residue, and effective mass may be obtained by Taylor expanding the retarded self-energy, $\Sigma^R(\mathbf{k}, \omega) \equiv \Sigma(\mathbf{k}, i\omega_m \rightarrow \omega + i0^+)$, near $\mathbf{k} = \mathbf{0}$ and $\omega = 0$. By substituting the expansion into the retarded impurity

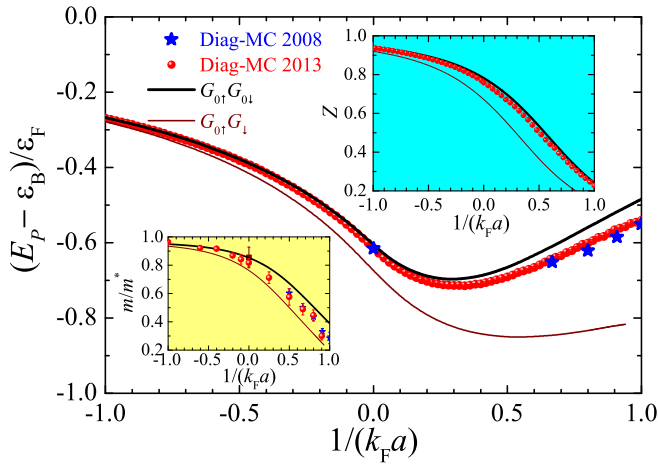


FIG. 2. (color online). The energy of attractive Fermi polarons (with the two-particle bound state energy $\epsilon_B = -\hbar^2/(ma^2) < 0$ subtracted on the BEC side), as a function of the interaction strength $1/(k_F a)$, obtained by the non-self-consistent T -matrix theory (thick black line) and self-consistent T -matrix theory (thin brown line) at $T = 0.01T_F$, and by diagrammatic Monte Carlo simulations at zero temperature in 2008 (blue stars) [8] and 2013 (red circles) [9]. The upper and lower insets show the residue and (inverse) effective mass of polarons, respectively.

Green's function, we find that,

$$E_P = (1 - Z) \mu_\downarrow + Z \text{Re} \Sigma^R(0, 0), \quad (13)$$

$$Z = \left(1 - \frac{\partial \text{Re} \Sigma^R}{\partial \omega} \right)^{-1}, \quad (14)$$

$$\frac{m}{m^*} = \left(1 + \frac{\partial \text{Re} \Sigma^R}{\partial \epsilon_{\mathbf{k}}} \right) \left(1 - \frac{\partial \text{Re} \Sigma^R}{\partial \omega} \right)^{-1}, \quad (15)$$

$$\gamma = -2Z \text{Im} \Sigma^R(0, 0). \quad (16)$$

As the impurity concentration is given by,

$$n_\downarrow = \sum_{\mathbf{k}} \int d\omega f(\omega) A_\downarrow(\mathbf{k}, \omega), \quad (17)$$

$$\simeq \sum_{\mathbf{k}} Z f \left(E_P + \frac{\hbar^2 \mathbf{k}^2}{2m^*} - \mu_\downarrow \right), \quad (18)$$

where $f(x) = 1/(e^x + 1)$ is the Fermi distribution, it is easy to see that at zero temperature we must have the identity $E_P = \mu_\downarrow$ for a single impurity at a vanishingly small density $n_\downarrow \simeq 0$ [7]. By using Eq. (13), we obtain the condition

$$\mu_\downarrow = \text{Re} \Sigma^R(0, 0), \quad (19)$$

which determines the impurity chemical potential for a single impurity at zero temperature [7–9].

It is worth mentioning that numerically it is difficult to directly take the analytical continuation $i\omega_m \rightarrow \omega + i0^+$ of the retarded self-energy. At low temperatures, where $\omega_m \equiv (2m + 1)\pi k_B T$ is small for small integers

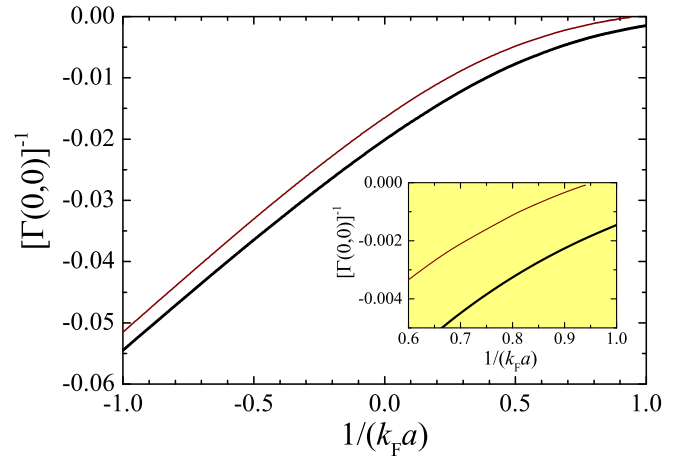


FIG. 3. (color online). The inverse of the impurity vertex function at zero momentum and zero frequency at $T = 0.01T_F$, in units of $2mk_F$, as a function of the interaction strength $1/(k_F a)$, obtained by using the non-self-consistent T -matrix theory (thick black line) and self-consistent T -matrix theory (thin brown line). The self-consistent theory predicts a pairing instability at the critical interaction strength $1/(k_F a)_c \simeq 0.95$, very close to the Diag-MC prediction $1/(k_F a)_c \simeq 0.9$ [8, 9]. The inset is an enlarged view near the critical interaction strength.

$m = 0, 1, 2$, we Taylor expand the self-energy around zero frequency, i.e.,

$$\Sigma(\mathbf{k}, i\omega_m) \simeq \Sigma^R(\mathbf{k}, 0) + \frac{\partial \Sigma^R}{\partial \omega}(i\omega_m), \quad (20)$$

or

$$\text{Re} \Sigma(\mathbf{k}, i\omega_m) \simeq \text{Re} \Sigma^R(\mathbf{k}, 0) - \frac{\partial \text{Im} \Sigma^R}{\partial \omega} \omega_m, \quad (21)$$

$$\text{Im} \Sigma(\mathbf{k}, i\omega_m) \simeq \text{Im} \Sigma^R(\mathbf{k}, 0) + \frac{\partial \text{Re} \Sigma^R}{\partial \omega} \omega_m, \quad (22)$$

and obtain $\Sigma^R(\mathbf{k}, 0)$ and $[\partial \Sigma^R(\mathbf{k}, \omega)/\partial \omega]_{\omega=0}$ by numerical extrapolation. An example of such an extrapolation is shown in Fig. 1 for an attractive polaron in the unitary limit. Consequently, we take the zero momentum limit and calculate the numerical derivative of the retarded self-energy with respect to $\epsilon_{\mathbf{k}}$ at $\mathbf{k} = 0$.

III. FERMI POLARONS AT ZERO TEMPERATURE: A BRIEF REVIEW

We have calculated the polaron energy, residue, and inverse effective mass as a function of the impurity-medium interaction strength at nearly zero temperature, by using both non-self-consistent and self-consistent T -matrix theories. These results were obtained earlier as a by-product in a zero-temperature Diag-MC simulation [9], although the predicted polaron energy from the self-consistent T -matrix theory was not explicitly reported.

As shown in Fig. 2, our results summarize the known quasi-particle properties of attractive Fermi polarons at zero temperature. For the polaron energy and residue, the prediction of the non-self-consistent T -matrix theory agrees well with the numerically exact Diag-MC simulations [8, 9]. The self-consistent T -matrix theory seems to underestimate the polaron energy and residue, in particular on the BEC side, where the scattering length is positive, $a > 0$. The Diag-MC results for the inverse effective mass lies between the predictions of the non-self-consistent and self-consistent T -matrix theories, as shown in the inset at the left bottom of Fig. 2. Overall, it is reasonable to believe that the non-self-consistent T -matrix theory works better than the self-consistent theory for attractive Fermi polarons at low temperature and small impurity concentration. However, in some cases the self-consistent theory may provide more useful information than the non-self-consistent theory. An interesting example is the polaron-molecule transition, which has been predicted by Diag-MC simulations to occur at about $1/(k_F a)_c \simeq 0.9$ [8, 9].

Indeed, the self-consistent T -matrix theory can be used to determine the instability of attractive Fermi polarons, with respect to the formation of a tightly bound molecular state of an impurity atom and a medium atom, due to their strong attraction. Numerically, we find that beyond a threshold interaction strength $1/(k_F a)_c \simeq 0.95$, the vertex function at zero momentum and frequency becomes positive, as shown in Fig. 3 (thin lines). Our numerical procedure for self-consistent calculations of the impurity Green's function and vertex function then breaks down. Physically, it signifies the condensation of spontaneously created molecules, following the so-called Thouless criterion for superfluidity [39],

$$\Gamma(\mathbf{q} = 0, i\nu_n = 0) = 0, \quad (23)$$

which is satisfied at the critical temperature T_c or critical interaction strength $1/(k_F a)_c$. The critical interaction strength $1/(k_F a)_c \simeq 0.95$ predicted by the self-consistent T -matrix theory is comparable to the critical value obtained by Diag-MC simulations [8, 9], in comparison, the non-self-consistent T -matrix theory predicts a much larger critical interaction strength (not shown in the figure).

IV. FERMI POLARONS AT FINITE TEMPERATURE

We now turn to consider the quasi-particle properties of attractive Fermi polarons at finite temperature. Figure 4 reports the polaron energy as a function of the reduced temperature T/T_F on the BCS side ($1/k_F a = -0.5$), in the unitary limit ($1/k_F a = 0$), and on the BEC side ($1/k_F a = +0.5$), obtained by using the non-self-consistent (a) and self-consistent (b) T -matrix theories. At low temperatures, i.e. $T < 0.05T_F$, the polaron energy decreases with increasing temperature. From the

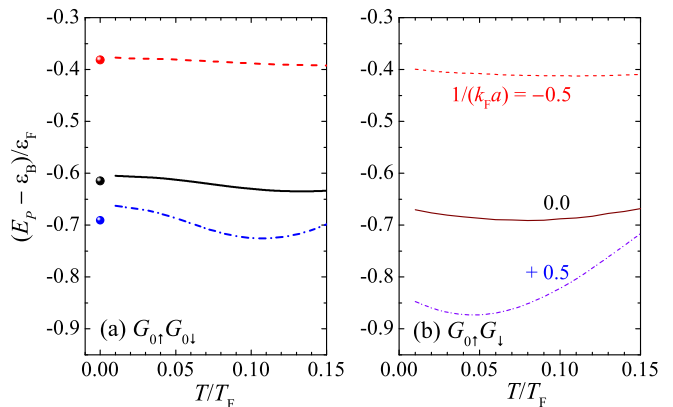


FIG. 4. (color online) Temperature dependence of the polaron energy at the impurity concentration $x = n_{\downarrow}/n = 0.01$ and at $1/(k_F a) = -0.5$ (dashed line), 0 (solid line), and 0.5 (dot-dashed line), calculated by using the non-self-consistent T -matrix theory (a, left panel) and self-consistent T -matrix theory (b, right panel). The circles in (a) show the diagrammatic Monte Carlo result [9].

viewpoint of one-particle-hole excitations, this decrease may arise from the enlarged phase space for particle-hole excitations at low temperature, and hence, the impurity is dressed by more particle-hole excitations. At temperatures near $T \sim 0.1T_F$ the polaron energy increases as the temperature increases. This increase can be clearly seen on the BEC side by using the self-consistent T -matrix theory, where the temperature-induced variation of the polaron energy is about $0.1\epsilon_F$ for $T < 0.15T_F$. Unfortunately, the current experimental measurement of the polaron energy is not accurate enough to resolve this variation. On the BCS side the temperature dependence of the polaron energy is typically weak and is only about a few percent of the Fermi energy. Both non-self-consistent and self-consistent T -matrix theories predict a similar polaron energy, due to the weak attraction.

Figure 5 shows the temperature dependence of the inverse effective mass (a, b) and the residue (c, d) of attractive Fermi polarons. These two quantities increase with increasing temperature, as predicted by both T -matrix theories. At $T > 0.05T_F$, this may be simply understood from the fact that with increasing temperature the polaron starts to lose its polaronic character and become more like an isolated impurity. As the temperature increases, the polarons effective mass approaches the bare mass m and its residue tends towards unity.

As a well-defined quasi-particle, an attractive Fermi polaron has infinitely long lifetime at zero temperature, unless a decay channel to the ground-state of molecules is opened above the critical interaction strength, $1/(k_F a)_c \sim 0.9$ [40]. At finite temperature, however, a Fermi polaron could decay via thermal excitations at arbitrary interaction strengths, where the decay rate is anticipated to be proportional to $(T/T_F)^2$ at low temperature [18]. In Fig. 6, we present the temperature dependence of the decay rate of attractive Fermi

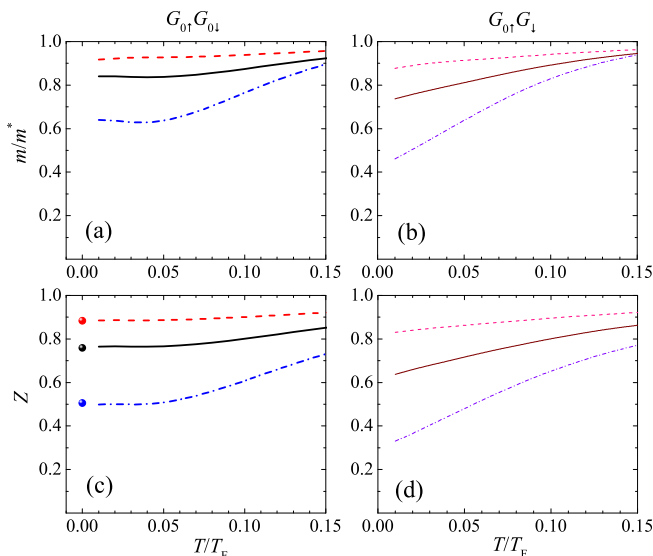


FIG. 5. (color online) Temperature dependence of the polaron effective mass (a, b) and residue (c, d) at the impurity concentration $x = n_{\downarrow}/n = 0.01$ calculated by using the non-self-consistent T -matrix theory (left panel) and self-consistent T -matrix theory (right panel). From top to bottom, the interaction strengths are $1/(k_F a) = -0.5$ (dashed line), 0 (solid line), and 0.5 (dot-dashed line). The circles in (c) show the diagrammatic Monte Carlo result [9].

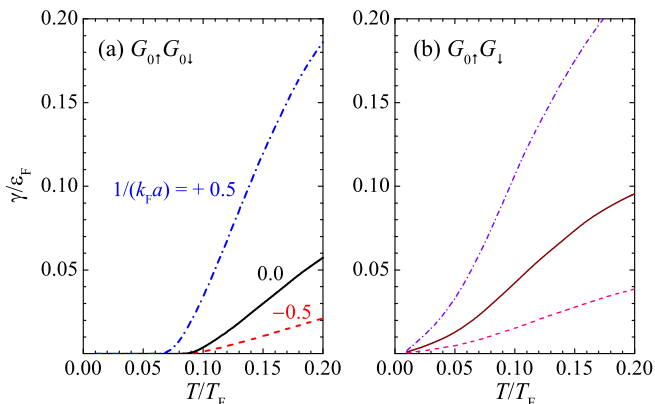


FIG. 6. (color online) Thermal-induced polaron decay rate at the impurity concentration $x = n_{\downarrow}/n = 0.01$ and at $1/(k_F a) = -0.5$ (dashed line), 0 (solid line), and 0.5 (dot-dashed line), calculated by using the non-self-consistent T -matrix theory (a, left panel) and self-consistent T -matrix theory (b, right panel).

polarons, calculated from the non-self-consistent (a) and self-consistent (b) T -matrix theories. On the BCS side, or near the unitary limit, the polaron decay rate is less than six percent of the Fermi energy at the temperature range considered (i.e., $T < 0.2T_F$). In contrast, on the BEC side, the thermal-induced decay becomes significant, where it can be as large as $0.1\epsilon_F$ at the typical experimental temperature of $T \sim 0.15T_F$. We note that, the decay rate determined by the self-consistent theory

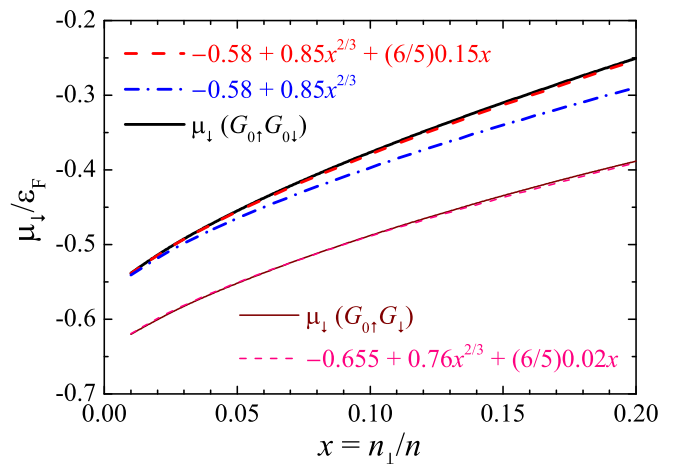


FIG. 7. (color online) The impurity chemical potential as a function of the impurity concentration x in the unitary limit ($1/k_F a = 0$) and at $T = 0.01T_F$, calculated by using the non-self-consistent T -matrix theory (thick black line) and the self-consistent T -matrix theory (thin brown line). The two red dashed lines are the fitting curve of the formula, $\mu_{\downarrow} = E_P + (m/m^*)x^{2/3} + (6/5)\mathcal{F}x$, where \mathcal{F} is the Landau parameter characterizing the polaron-polaron interaction. The dot-dashed line illustrates the importance of the polaron-polaron interaction term $(6/5)\mathcal{F}x$.

is larger than the non-self-consistent theory. Moreover, the non-self-consistent theory seems to predict a threshold temperature (i.e., $T \sim 0.08T_F$), below which there is no notable decay.

V. FERMI POLARONS AT FINITE IMPURITY DENSITY

In this section, we consider the quasi-particle properties of attractive Fermi polarons at finite impurity concentration/density and discuss their density dependence at both essentially zero temperature (i.e., $T = 0.01T_F$) and finite temperature. At the end of the section, we also make a comparison with the first Fermi polaron experiment [18].

A. Fermi liquid behavior

At low impurity concentration and low temperatures, Fermi polarons are believed to form a Fermi liquid [4, 5]. In the spirit of Landau's Fermi liquid theory, the change in the total energy due to the addition of impurity atoms with density $x = n_{\downarrow}/n = N_{\downarrow}/N$, where N_{\downarrow} and N are respectively the number of impurity atoms and medium atoms, can be written in an energy functional with two density dependent terms [4, 5],

$$\Delta E \simeq N_{\downarrow}E_P + \frac{3}{5}N\epsilon_F \left[\frac{m}{m^*} \left(\frac{N_{\downarrow}}{N} \right)^{5/3} + \mathcal{F} \frac{N_{\downarrow}^2}{N^2} \right], \quad (24)$$

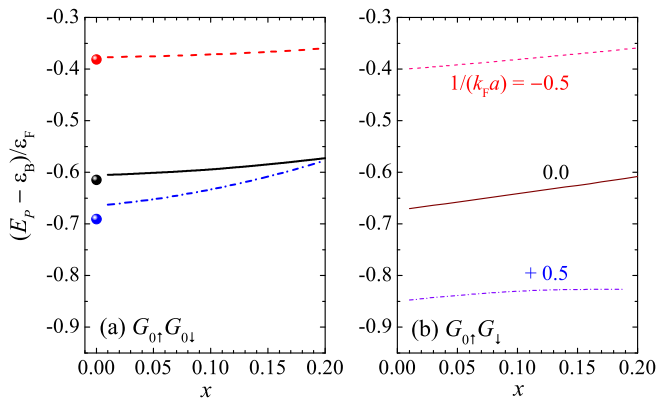


FIG. 8. (color online) The polaron energy as a function of the impurity concentration x at $T = 0.01T_F$ and at three different interaction strengths: $1/(k_F a) = -0.5$ (dashed line), 0 (solid line), and 0.5 (dot-dashed line), calculated by using the non-self-consistent T -matrix theory (a, left panel) and self-consistent T -matrix theory (b, right panel). The circles in (a) show the diagrammatic Monte Carlo result [9].

where $E_P(T)$ and $m^*(T)$ are respectively the polaron energy and effective mass of a *single* impurity at low temperature T . The term proportional to m/m^* in the bracket accounts for the Fermi pressure of the quasi-particle polaron gas, while the second term with a *defined* Landau parameter \mathcal{F} may be viewed as the interaction energy arising from the effective polaron-polaron interaction. By taking the partial derivative with respect to the impurity density, $\partial\Delta E/\partial N_\downarrow = \mu_\downarrow$, the impurity chemical potential is given by,

$$\mu_\downarrow = E_P(T) + \frac{m}{m^*(T)}x^{2/3}\varepsilon_F + \frac{6}{5}\mathcal{F}(T)x\varepsilon_F + \dots \quad (25)$$

it is important to note that the Landau parameter \mathcal{F} is always positive and is an effective *repulsive* polaron-polaron interaction. In Fig. 7, we check the Fermi liquid description by using the non-self-consistent (upper thick line) and self-consistent (lower thin line) T -matrix theories in the unitary limit. We fit the calculated impurity chemical potential with Eq. (25) and then extract the polaron energy E_P , inverse effective mass m/m^* and Landau parameter \mathcal{F} . The extracted energy and effective mass agree well with these calculated via Eq. (13) and Eq. (14) at the same temperature $T = 0.01T_F$. In addition, in the case of the non-self-consistent T -matrix theory, the extracted Landau parameter $\mathcal{F} \simeq 0.15$ is close to the value of $\mathcal{F} = 0.20$ calculated using the same ladder approximation [22] or the prediction $\mathcal{F} = 0.14$ from the fixed-node diffusion Monte Carlo [5].

B. Density dependence of the polaron energy, mass and residue

We now consider the density dependence of the quasi-particle properties of attractive Fermi polarons at zero

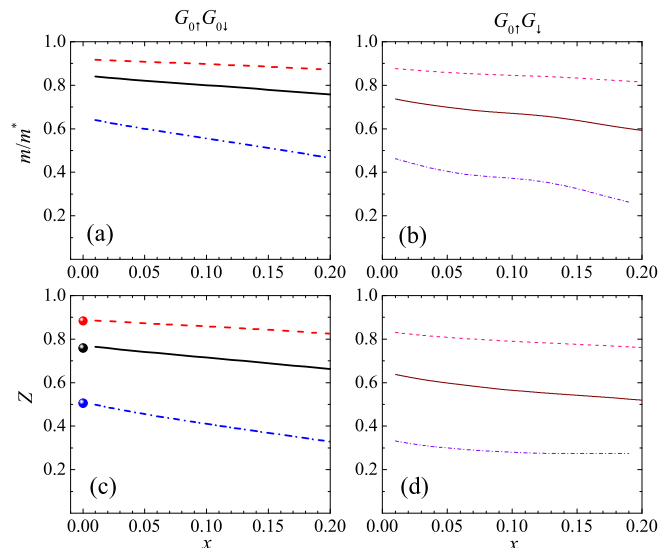


FIG. 9. (color online) The inverse effective mass (a, b) and the residue (c, d) of attractive Fermi polarons as a function of the impurity concentration x at $T = 0.01T_F$ and at different interaction strengths: $1/(k_F a) = -0.5$ (dashed line), 0 (solid line), and 0.5 (dot-dashed line), calculated by using the non-self-consistent T -matrix theory (left panel) and self-consistent T -matrix theory (right panel). The circles in (c) show the diagrammatic Monte Carlo result [9].

temperature. It is useful to note that, the impurity chemical potential is equivalent to the polaron energy only at zero temperature for a single impurity [7]. In general, the polaron energy defined by Eq. (12) is different from the impurity chemical potential. In particular, we anticipate that the polaron energy is not affected by the many-body effect of the Fermi pressure term, that is the term $\propto (m/m^*)x^{2/3}$ in the impurity chemical potential, Eq. (25). However, the polaron energy may be affected by the residual interaction between polarons.

Figure 8 reports the density dependence of the polaron energy at three typical interaction strengths and at $T = 0.01T_F$, determined by using the two T -matrix theories. As anticipated, the polaron energy does not show the existence of the Fermi pressure term, which otherwise will lead to a strong density dependence. The slight increase in the polaron energy with increasing density, predicted by both theories, could be attributed to the residual polaron-polaron interaction. According to the non-self-consistent T -matrix theory [22], with increasing interaction parameter, the Landau parameter \mathcal{F} is small on the BCS side, takes a maximum at $1/(k_F a) \sim 0.6$ and finally becomes small again in the BEC limit. As shown in Fig. 8a, the slopes of the polaron energy as a function of the density x at different interaction strengths are consistent with the interaction dependence of the Landau parameter \mathcal{F} .

Figure 9 presents the density dependence of the inverse effective mass and residue of Fermi polarons at $T = 0.01T_F$. Both quantities decrease with increas-

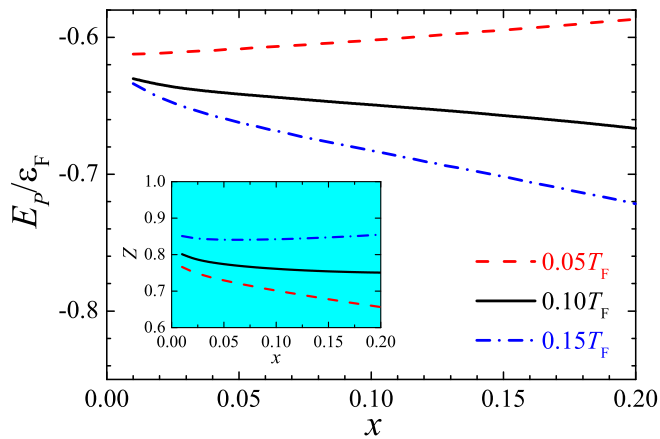


FIG. 10. (color online) The polaron energy as a function of the impurity concentration x in the unitary limit and at three different temperatures: $T = 0.05T_F$ (red dashed line), $0.10T_F$ (black solid line) and $0.15T_F$ (blue dot-dashed line). The inset shows the polaron residue.

ing density, suggesting that the polaronic character is amplified by a finite density. A reduced polaron residue at nonzero impurity concentration is qualitatively consistent with the experimental measurement [18]. For example, in the unitary limit it was experimentally observed that $Z = 0.39(9)$ at 5% impurity concentration [18], smaller than the variational prediction of $Z \simeq 0.78$ for a single impurity [6, 7]. However, our results at $x = 0.05$, i.e., $Z \simeq 0.74$ from the non-self-consistent theory and $Z \simeq 0.60$ from the self-consistent theory, can not quantitatively explain the experimental finding.

C. Density dependence of the polaron energy and residue at finite temperature

We now discuss the polaron quasi-particle properties at both nonzero temperature and nonzero impurity concentration. Figure 10 shows the polaron energy (main figure) and the residue (inset) as a function of the impurity concentration at three different temperatures: $T = 0.05T_F$ (dashed line), $0.10T_F$ (solid line), and $0.15T_F$ (dot-dashed line). It is interesting that the density dependence qualitatively changes at higher temperatures. For instance, at $T = 0.15T_F$ the polaron energy appears to decrease with increasing density, while the polaron residue starts to increase. Physically, a reduced polaron energy at nonzero impurity density indicates an *attractive* effective interaction between polarons. Thus, we conclude that the effective polaron-polaron interaction may change its sign with increasing temperature.

At high temperature, where the polaron becomes more likely an individual, isolated impurity, the attractive polaronic interaction could be understood from the induced interaction due to the exchange of medium atoms. For a weak impurity-medium interaction U , it is well known

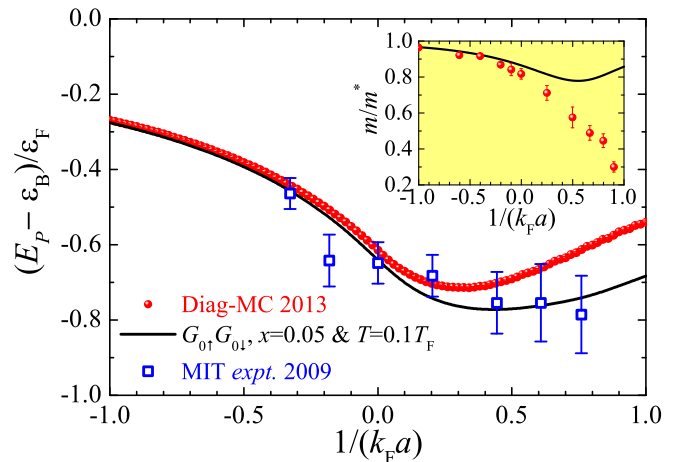


FIG. 11. (color online) The polaron energy at finite temperature $T = 0.10T_F$ and at nonzero impurity concentration $x = 0.05$, determined by using the non-self-consistent T -matrix theory (black solid line). For comparison, we show also the diagrammatic Monte Carlo results at zero temperature (red circles) [9] and the experimental data on ${}^6\text{Li}$ atoms at similar temperature and impurity concentration (i.e., $T_{\text{expt}} = 0.14(3)T_F$ and $x_{\text{expt}} \simeq 0.05$, blue empty squares) [18]. The latter is extracted from the review article [2].

that such an exchange process leads to an induced interaction [41, 42]

$$U_{\text{ind}} = -U^2 \chi(\mathbf{q}, \omega), \quad (26)$$

which should be attractive. Here $\chi(\mathbf{q}, \omega)$ is the density-density response function of the medium atoms with momentum \mathbf{q} and frequency ω [41, 42]. Our results of a temperature-dependent polaron-polaron interaction suggest that the weak-coupling picture of induced interactions should be improved close to zero temperature, in order to accommodate a repulsive effective interaction between polarons.

D. Comparison with Fermi polaron experiments

An attractive polaron-polaron interaction at nonzero temperature may lead to a sizable down-shift in the polaron energy at finite impurity concentration. To show this we report in Fig. 11 the polaron energy at $T = 0.10T_F$ and $x = 0.05$, across the whole the BCS-BEC crossover, calculated by using the non-self-consistent T -matrix theory. The inverse effective mass is shown in the inset. It is readily seen that the correction due to the combined effect of temperature and impurity concentration is negligible on the BCS side and in the unitary limit. However, the correction becomes increasingly pronounced on the BEC side. The down-shift in the polaron energy is typically about $0.1 \sim 0.2\varepsilon_F$, and more impressively the inverse effective mass m/m^* becomes less dependent on the interaction parameter $1/(k_F a)$, staying around $m/m^* \simeq 0.8 \sim 0.9$.

We now make a comparison with the first attractive Fermi polaron experiment [18]. The experiment was carried out at similar temperature (i.e., $T_{\text{expt}} = 0.14(3)T_F$) and impurity concentration ($x_{\text{expt}} \simeq 0.05$). It is encouraging to see that our theoretical prediction of the polaron energy fits well with the measured data (empty squares with error bars) [18], better than the Diag-MC results for a single impurity at zero-temperature (solid circles) [9], significantly on the BEC side of the interaction.

Our result of an interaction-insensitive effective mass at finite temperature is useful to understand the *weak* density dependence of the rf peak positions for the attractive branch [18]. Experimentally, the polaron energies $E_{P\pm}$ for both attractive and repulsive polarons are measured from the peak position Δ_{\pm} of the rf-spectroscopy [22],

$$\Delta_{\pm} = E_{P\pm} - \left(1 - \frac{m}{m^*}\right) \bar{\varepsilon}, \quad (27)$$

where the second term on the right-hand-side of the equation reflects the different dispersion relation of an impurity in the polaron state and in the third free hyperfine state, and where $\bar{\varepsilon} = \langle \hbar^2 \mathbf{k}^2 / (2m) \rangle$ is the mean kinetic energy per impurity due to the finite impurity concentration $x \neq 0$ (see Eq. (12)). Therefore, if the effective mass m^* of Fermi polarons differs notably from the bare mass m (i.e., $1 - m/m^* \gg 0$), one can measure m/m^* from the dependence of Δ_{\pm} on $\bar{\varepsilon}$. This protocol works very well for repulsive Fermi polarons of ${}^6\text{Li}$ atoms [22]. However, it does not work for attractive Fermi polarons [18], although the variational theory predicts small enough m/m^* for both repulsive and attractive Fermi polarons at about $1/(k_{Fa}) \sim 0.6$ at *zero* temperature [22]. As shown in the inset of Fig. 11, the inverse effective mass of attractive Fermi polarons at finite temperature actually differs significantly from its zero temperature value on the experimentally relevant BEC side. The quantity $1 - m/m^*$ is close to zero and the resulting weak dependence of Δ_{-} on $\bar{\varepsilon}$ shows experimentally it will be difficult to extract m/m^* .

VI. CONCLUSIONS

In summary, we have presented a systematic investigation of the effects of finite temperature and finite impurity concentration on the quasi-particle properties of attractive Fermi polarons. On the BEC side beneath the Feshbach resonance of the impurity and medium atoms, we have found that a nonzero temperature, as small as one-tenth of the Fermi temperature, may lead to a sizable correction to the polaron energy. In this regime the effective mass of attractive polarons can be reduced significantly, leading to a weak dependence of the measured resonance peak in the radio-frequency spectroscopy on the impurity concentration. These results have been used to better understand the first Fermi polaron experiment carried out at MIT in 2009 [18].

It will be interesting to extend our study to the case of repulsive Fermi polarons and consider the temperature effect in the recent LENS experiment with ${}^6\text{Li}$ atoms [22]. To do so, we need to solve the coupled T -matrix equations Eqs. (4), (5), (6) and (7) in the real-frequency domain and determine the single-particle spectral function of the impurity. Our many-body T -matrix theories may also be extended to address the possible finite temperature effect in Bose polarons, which have been recently experimentally investigated [23, 24].

ACKNOWLEDGMENTS

We thank very much Kris Van Houcke for kindly sharing their Diag-MC data in Ref. [9] with us. HH and XJL acknowledges the hospitality of Institute for Advanced Study at Tsinghua University, where a part of the work was done during their visit. Our research was supported by Australian Research Council's (ARC) Discovery Projects: DP140100637 and FT140100003 (XJL), FT130100815 and DP170104008 (HH).

-
- [1] I. Bloch, J. Dalibard, and W. Zwerger, *Rev. Mod. Phys.* **80**, 885 (2008).
 - [2] For a recent review, see, for example, P. Massignan, M. Zaccanti, and G. M. Bruun, *Rep. Prog. Phys.* **77**, 034401 (2014).
 - [3] C. Chin, R. Grimm, P. Julienne, and E. Tiesinga, *Rev. Mod. Phys.* **82**, 1225 (2010).
 - [4] C. Lobo, A. Recati, S. Giorgini, and S. Stringari, *Phys. Rev. Lett.* **97**, 200403 (2006).
 - [5] S. Pilati and S. Giorgini, *Phys. Rev. Lett.* **100**, 030401 (2008).
 - [6] F. Chevy, *Phys. Rev. A* **74**, 063628 (2006).
 - [7] R. Combescot, A. Recati, C. Lobo, and F. Chevy, *Phys. Rev. Lett.* **98**, 180402 (2007).
 - [8] N. Prokof'ev and B. Svistunov, *Phys. Rev. B* **77**, 020408(R) (2008).
 - [9] J. Vlietinck, J. Ryckebusch, and K. Van Houcke, *Phys. Rev. B* **87**, 115133 (2013).
 - [10] P. Kroiss and L. Pollet, *Phys. Rev. B* **91**, 144507 (2015).
 - [11] R. Combescot and S. Giraud, *Phys. Rev. Lett.* **101**, 050404 (2008).
 - [12] X. Cui and H. Zhai, *Phys. Rev. A* **81**, 041602(R) (2010).
 - [13] W. Li and S. Das Sarma, *Phys. Rev. A* **90**, 013618 (2014).
 - [14] J. Levinsen, M. M. Parish, and G. M. Bruun, *Phys. Rev. Lett.* **115**, 125302 (2015).
 - [15] Y. Nishida, *Phys. Rev. Lett.* **114**, 115302 (2015).
 - [16] W. Yi and X. Cui, *Phys. Rev. A* **92**, 013620 (2015).
 - [17] M. Sun, H. Zhai, and X. Cui, *Phys. Rev. Lett.* **119**, 013401 (2017).
 - [18] A. Schirotzek, C.-H. Wu, A. Sommer, and M.W. Zwier-

- lein, Phys. Rev. Lett. **102**, 230402 (2009).
- [19] Y. Zhang, W. Ong, I. Arakelyan, and J. E. Thomas, Phys. Rev. Lett. **108**, 235302 (2012).
- [20] C. Kohstall, M. Zaccanti, M. Jag, A. Trenkwalder, P. Massignan, G.M. Bruun, F. Schreck, and R. Grimm, Nature (London) **485**, 615 (2012).
- [21] M. Koschorreck, D. Pertot, E. Vogt, B. Fröhlich, M. Feld, and M. Köhl, Nature (London) **485**, 619 (2012).
- [22] F. Scazza, G. Valtolina, P. Massignan, A. Recati, A. Amico, A. Burchianti, C. Fort, M. Inguscio, M. Zaccanti, and G. Roati, Phys. Rev. Lett. **118**, 083602 (2017).
- [23] M.-G. Hu, M. J. Van de Graaff, D. Kedar, J. P. Corson, E. A. Cornell, and D. S. Jin, Phys. Rev. Lett. **117**, 055301 (2016).
- [24] N. B. Jørgensen, L. Wacker, K. T. Skalmstang, M. M. Parish, J. Levinsen, R. S. Christensen, G. M. Bruun, and J. J. Arlt, Phys. Rev. Lett. **117**, 055302 (2016).
- [25] E. V. H. Doggen and J. J. Kinnunen, Phys. Rev. Lett. **111**, 025302 (2013).
- [26] For an application of Chevy's variation approach at finite temperature, see, M. Parish and J. Levinsen, Phys. Rev. B **94**, 184303 (2016).
- [27] P. Massignan, G. M. Bruun, and H. T. C. Stoof, Phys. Rev. A **77**, 031601(R) (2008).
- [28] M. Punk, P. T. Dumitrescu, and W. Zwerger, Phys. Rev. A **80**, 053605 (2009).
- [29] P. Massignan and G. M. Bruun, Eur. Phys. J. D **65**, 83 (2011).
- [30] R. Schmidt, T. Enss, V. Pietilä, and E. Demler, Phys. Rev. A **85**, 021602(R) (2012).
- [31] J. E. Baarsma, J. Armaitis, R. A. Duine, and H. T. C. Stoof, Phys. Rev. A **85**, 033631 (2012).
- [32] R. Haussmann, Phys. Rev. B **49**, 12975 (1994).
- [33] X.-J. Liu and H. Hu, Phys. Rev. A **72**, 063613 (2005).
- [34] R. Haussmann W. Rantner, S. Cerrito, and W. Zwerger, Phys. Rev. A **75**, 023610 (2007).
- [35] S. P. Rath and R. Schmidt, Phys. Rev. A **88**, 053632 (2013).
- [36] V. M. Loktev, R. M. Quick, and S. G. Sharapov, Phys. Rep. **349**, 1 (2001).
- [37] H. Hu, X.-J. Liu, and P. D. Drummond, Phys. Rev. A **77**, 061605 (2008).
- [38] B. C. Mulkerin, K. Fenech, P. Dyke, C. J. Vale, X.-J. Liu, and H. Hu, Phys. Rev. A **92**, 063636 (2015).
- [39] P. Nozières and S. Schmitt-Rink, J. Low Temp. Phys. **59**, 195 (1985).
- [40] G. M. Bruun and P. Massignan, Phys. Rev. Lett. **105**, 020403 (2010).
- [41] H. Heiselberg, C. J. Pethick, H. Smith, and L. Viverit, Phys. Rev. Lett. **85**, 2418 (2000).
- [42] J. J. Kinnunen and G. M. Bruun, Phys. Rev. A **91**, 041605(R) (2015).